An Intracellular Study of the Contrast-Dependence of Neuronal Activity in Cat Visual Cortex

Bashir Ahmed, John D. Allison, Rodney J. Douglas and Kevan A.C. Martin

Institute of Neuroinformatics, ETH/UNIZ, Gloriastraße 32, Zürich CH-8006, Switzerland

Extracellular recordings indicate that mechanisms that control contrast gain of neuronal discharge are found in the retina, thalamus and cortex. In addition, the cortex is able to adapt its contrast response function to match the average local contrast. Here we examine the neuronal mechanism of contrast adaptation by direct intracellular recordings *in vivo*. Both simple ($n = 3$) and complex cells ($n = 4$) show contrast adaptation during intracellular recording. For simple cells, that the amplitude of fluctuations in membrane potential induced by a drifting grating stimulus follows a contrast response relation similar to lateral geniculate relay cells, and does not reflect the high gain and adaptive properties seen in the action potential discharge of the neurons. We found no evidence of significant shunting inhibition that could explain these results. In complex cells there was no change in the mean membrane potential for different contrast stimuli or different states of adaptation, despite marked changes in discharge rate. We use a simplified electronic model to discuss the central features of our results and to explain the disparity between the contrast response functions of the membrane potential and action potential discharge in simple cells.

Introduction

Significant transformations in the coding and representation of visual stimuli occur at different levels along the pathway from photoreceptors to the primary visual cortex. For example, the increased stimulus selectivity of cortical neurons relative to their retinal and thalamic antecedents is particularly evident and has been intensively studied, although the mechanisms by which cortical neurons become selective remain hotly debated (e.g. Das, 1996; Vidyasagar *et al.*, 1996). There is agreement, however, that the selectivity of cortical neurons remains stable in the face of noise, which arises from many internal sources as well as the external stimulus itself. One simple example of this stability is the invariance of the orientation tuning of cortical neurons in the face of large variations in the contrast of a stimulus (Sclar and Freeman, 1982). The contrast invariance of the orientation tuning of cortical neurons reflects the relative perceptual importance of form versus absolute contrast. However, it also implies that the changes in neural activity induced by changes in the intensity (i.e. contrast) of a stimulus are being precisely registered and compensated for so that activity changes induced by changes in the form of the stimulus can be explicitly monitored. Alternatively, the compensation for stimulus contrast can be interpreted as suppression of 'noise'.

In order to understand how cortical neurons perform the computations underlying operations like contrast invariant orientation tuning, it is important to understand the constraints of the 'wetware' that carries out these computations. The cortex is not a Turing Universal Machine. It has to perform many different functions in real time and cannot be rapidly reprogrammed to perform each different algorithm as it is required. It is not hard-wired but 'firm-wired'; i.e. changes in wiring do occur, but more slowly than the time needed to carry out a particular computation. It would seem that the comprehensive solution to the computation of multiple functions must come through the operation of a collection of separate circuits that carry out separate dedicated algorithms in parallel. This view has been strongly pursued in recent years (Livingstone and Hubel, 1988; Zeki and Shipp, 1988; VanEssen *et al.*, 1992). However, the original experimental evidence of Hubel and Wiesel (1962) shows that multiple functions are carried out by the same basic circuits: individual neurons are simultaneously direction selective, velocity tuned, orientation selective, disparity selective and so forth. Thus, there may not be a distinct separation between the circuits that process different attributes of the stimulus. Unfortunately, we presently do not understand how the microcircuits are organized to perform these most basic computations, or how these multiple computations are synthesized.

Over the past decade we have been actively developing and exploring, both theoretically and experimentally, the possibility of generating a unifying model of cortical microcircuits, within which these different functions can be reconciled. The form of the microcircuit, based on explorations of cat visual cortex, is that a column of neurons are connected in recurrent excitatory and inhibitory circuits (Douglas *et al.*, 1989; Douglas and Martin, 1991). These recurrent circuits are used to amplify the relatively small input signal provided by the thalamus or any other distant source. Whether a given pattern of input signals is amplified or inhibited is determined both by the pattern of connections between the thalamus and the cortical neurons and by the local pattern of connections between the cortical neurons themselves. Thus, the recurrent circuit provides a means of changing the gain of the excitatory feedback to individual neurons. It is a selectivity of gain control that provides a necessary basic mechanism for cortical computations. Theoretical and experimental studies have shown that this computational mechanism of gain modification is effective in explaining the behaviour of cortical neurons in such canonical problems as orientation selectivity, velocity tuning and direction selectivity (Douglas and Martin, 1991; Somers *et al.*, 1995; Suarez *et al.*, 1995; Maex and Orban, 1996).

That the same basic circuit can provide results that are not only consistent with the experimental data, but also cover such a broad range of problems is encouraging. However, much more remains to be explored in the domain of cortical amplification. For example, while great attention has been paid to transformations in the domain of pattern selectivity (see Martin, 1988, 1994), equally profound alterations are evident in the domain of the adaptive state of cortex (Albrecht and Hamilton, 1982; Ohzawa *et al.*, 1985; Bonds, 1991). It is evident from these studies that the responses of particular synapses, neurons or circuits are influenced by their history of stimulation. In this paper we explore, through experimental work and simulations,

Cerebral Cortex Sep 1997;7:559–570; 1047–3211/97/$4.00

some extensions of the model into the domain of contrast gain control and contrast adaptation, by which we mean the adjustment of the response of neurons to conform to the prevailing range and average of the stimulus contrast. This problem has been selected for study here because it is the best example of a history-dependent process in cortex, with sufficiently long time constants to be visible experimentally.

Contrast Gain Control

The retinal circuitry is exquisitely designed to measure local luminance while adjusting the operating range of the relevant neurons to prevent the saturation catastrophe (Shapley and Enroth-Cugell, 1984) that is so evident in equivalent artificial devices such as CCD cameras. In addition to the gain, which changes according to the mean flux, the retinal circuitry adapts its operating point to the average modulation of the luminance of the visual stimulus. This adjustment is usually referred to as contrast gain control (Shapley and Victor, 1978), where gain is defined as the ratio of the change in response to change in stimulus.

Mechanisms that control contrast gain are also found in the thalamus and cortex. The cortex has an additional mechanism that involves not simply a change in gain over a range of contrasts, but an adaptive resetting of the operating range proportional to the prevailing local contrast. Thus, the subcortical signal that carries information about contrast undergoes two changes. One is that for a given prevailing contrast the signal is amplified; and the other is that the operating range of the cortical neuron is continuously adjusted to match the prevailing contrast. As a result the response sensitivity of the cortical neuron to changes in contrast is maximized.

The form of the cortical contrast response function (CRF) during rapid changes in contrast is best described by the general hyperbolic ratio relationship, $F(c) = F_{max}c^n/(c^n + c_{50}{}^n)$, where F_{max} is the maximum discharge response of the cell, c_{50} is the semi-saturation constant and n is the steepness of slope, typically ~3.4 for monkey and 2.5 for cat area 17 (Albrecht and Hamilton, 1982). Variants of the hyperbolic ratio equation, such as the Naka–Rushton relationship (Naka and Rushton, 1966), were originally applied to retinal data, but have also been used to describe the contrast response of cortical neurons in cat and monkey (Albrecht *et al.*, 1984; McLean and Palmer, 1996). Gain control is a general property of cortical neurons, and the major contributions to the control arise from within the receptive field of the neuron (Ohzawa *et al.*, 1985). There is evidence that contrast gain adaptation operates down to as little as a few per cent of contrast (Ohzawa *et al.*, 1985; Bonds, 1991). This mechanism ensures that the dynamic range of cortical neurons is well matched to the range of contrast signal available in the current visual scene. An alternative interpretation is that the adaptation of contrast gain reflects a general method of common mode rejection and signal normalization in cortex.

The most circuit-based model of the contrast response of cortical cells is the *normalization model* proposed by Carandini and Heeger (1994). In their model the response of the cortical neurons is rescaled according to the contrast of the stimulus. This rescaling occurs through a feedback mechanism that drives an inhibitory shunt whose strength is proportional to the average activity of a pool of excitatory neurons. Thus, increasing stimulus contrast increases the conductance of the neuron and the spike output is reduced. This model replicates the form of the curve described by the Naka–Rushton equation, which provides the best fit to the experimental contrast-response function. In their model, the predicted increase in conductance induced by the shunting inhibitory feedback is considerable – ~4-fold for a full range of contrast. Such large changes in conductance have not been observed experimentally in any other visually evoked processes involving inhibition (Berman *et al.*, 1991; Pei *et al.*, 1991; Ferster and Jagadeesh, 1992). The presence of such a novel shunting inhibitory mechanism would require some distinct differences in the cortical circuits mediating contrast gain control as compared to those mediating orientation or direction selectivity, for example. An additional difficulty with the model is that the best candidate for the source of the shunting inhibition, the GABAa receptor, appears not to be involved in the process of adaptation since blocking it does not change the CRF (DeBruyn and Bonds, 1986; Vidyasagar, 1990; McLean and Palmer, 1996).

Although the contrast-dependent adaptation of the operating range seen by Ohzawa *et al.* (1982) and Albrecht *et al.* (1984) can be easily explained mathematically as a change in the semi-saturation constant of the Naka–Rushton relation (Albrecht *et al.*, 1984; Carandini and Heeger, 1994), the neuronal mechanism is unknown. In studies of contrast adaptation (Ohzawa *et al.*, 1982; Albrecht *et al.*, 1984), the form of the contrast-response function remained approximately constant after adaptation to different contrast levels, but the curves shifted progressively along the abscissae, i.e. the contrast axis, as the adapting contrast increased. Since the contrast axis is conventionally plotted in log units, such a shift indicates that the process underlying adaptation is multiplicative, i.e. an addition of logs. The time constant of the process is ~5–10 s (Albrecht *et al.*, 1984; Ohzawa *et al.*, 198; Bonds, 1991), which is several orders of magnitude slower than spike adaptation, or synaptic depression and synaptic potentiation, where the time constants are in the range of 10s of ms.

It is clear from the experimental work of Sclar and Freeman (1982), Ohzawa *et al.* (1982) and Albrecht *et al.* (1984) that the same machinery involved with processing form also shapes the response of neurons according to prevailing contrast. This is the challenge to our recurrent model, which so far has only dealt with form and motion processing. It is important that the contrast-dependent response of cortical neurons be expressed by the same microcircuit we have previously proposed. We have approached this problem using intracellular recording to examine the subthreshold and suprathreshold responses of cortical neurons to changes in contrast. In this paper we explore experimentally some of the possible mechanisms whereby the operating point might be changed. We have found no evidence that strong shunting inhibition is acting to shape the contrast response function or to adjust the operating point of cortical neurons. In explorations with a simple recurrent electronic circuit model it appears that these contrast-dependent changes in neuronal responses could be explained within the basic framework of the model we have previously developed. A preliminary abstract of this work has appeared previously (Allison *et al.*, 1996).

Methods

Surgery and Preparation

The basic procedures have been described in detail elsewhere (Martin and Whitteridge, 1984). Some minor modifications were the pre-operative sedation procedure of the s.c. injection of 0.3 cc acetylpromazine maleate (ACP, 10 mg/ml; C-VET, Bury St Edmunds, UK) followed by two i.m. injections of total volume 1.0 cc alphaxalone–

alphadolone (Saffan, 5 mg/ml; Pitman-Moore, Middlesex, UK). Full anaesthesia was induced with 2–3% halothane in a 70:30 N_2O/O_2 mixture and maintained during surgery with i.v. Saffan and 1% halothane in N_2O/O_2. EEG, ECG, arterial blood pressure, heart rate, expired CO_2 and rectal temperature were monitored continuously during the experiments. A small craniotomy was made over the postlateral gyrus at Horsely–Clarke AP coordinates –3 to –6 mm. The cat was then injected i.v. with muscle relaxants (gallamine triethiodide 80 mg induction, 13 mg/kg/h maintenance with tubocurarine) to stabilize the eyes. Saffan or pentobarbitol was given i.v. as needed to ensure the presence of frequent 'sleep spindles' in the EEG. The pupils were dilated with atropine sulphate and contact lenses were fitted; the eyes were refracted and corrected with lenses to focus on the display 57 cm distant. The location of the optic disk of each eye was plotted on a tangent screen with a reversible ophthalmoscope. At the termination of the recording the cat was injected i.v. with an overdose of sodium pentobarbital and perfused through the heart with fixatives.

Recording

Glass pipettes were filled with a solution of 4% horseradish peroxidase (HRP) in 0.2 M KCl buffered with 0.05 M Tris (pH 7.9), and bevelled to an impedance of 40–70 MΩ. Recordings were made with an HS-2A headstage preamplifier (Axon Instruments, Burlingame, CA) connected to an Axoprobe 1A amplifier. The membrane voltage recordings were filtered at 5 kHz, digitized at 10 kHz (CED 1401) recorded on disk for offline analysis using Spike2 software (Cambridge Electronic Design Ltd, Cambridge, UK).

In most cases, extracellular records were obtained before penetrating the cell. During this time, the receptive field was hand-plotted on a tangent screen and the optimal stimulus parameters, including orientation, spatial frequency and temporal frequency, were qualitatively determined with drifting sine wave gratings. Stimulus patterns were presented on a Tektronix 608 display (68 cd/m sq mean luminance) with a 10-deg-diameter circular CRT. Images were generated by a Picasso image synthesizer (InnisFree, Cambridgeshire, UK) controlled by VS software (Cambridge Electronic Design, Cambridge, UK) via a CED 1708 interface. Cells were classified as simple (S-type) or complex (C-type) on the basis of their receptive field structure (Hubel and Wiesel, 1962). Biophysical measurements were conventional.

Results

The data presented are from experiments on six adult female cats. We recorded intracellularly from single neurons and intra-axonally from terminal axons of dLGN relay cells in area 17. After plotting the receptive field of each neuron or axon, we made quantitative recordings with a computer-controlled stimulus. We used a modified version of the technique of Ohzawa *et al.* (1982, 1985) to measure the CRFs of individual geniculate axons or cortical neurons adapted to different stimulus contrast levels. Each neuron was pre-adapted by stimulating for 10 s with a drifting sine wave grating of contrast 7%, 28% or, in some cases, 56%. The contrast was then stepped to double (75% max.) or half its adapting value, or repeated at the adapting value, for 3 s. The step sequences were interleaved to give five trials at each contrast. Our recordings from dLGN afferent fibres confirmed previous observations that the CRFs of cat geniculate relay neurons extend over the entire contrast range and do not show the adaptive shifts in contrast-responses that are a feature of their cortical targets (Fig. 2) (Ohzawa *et al.*, 1985).

The cortical data discussed here are drawn from seven cells that were recorded for sufficiently long periods (>20 min) to enable the protocol to be applied at more than one adapting contrast. Three neurons had S-type (simple) receptive fields and four had C-type (complex). Single trials from one simple and one complex cell are shown in Figure 1 for comparison. The simple cell shows the typical modulated membrane fluctuations and

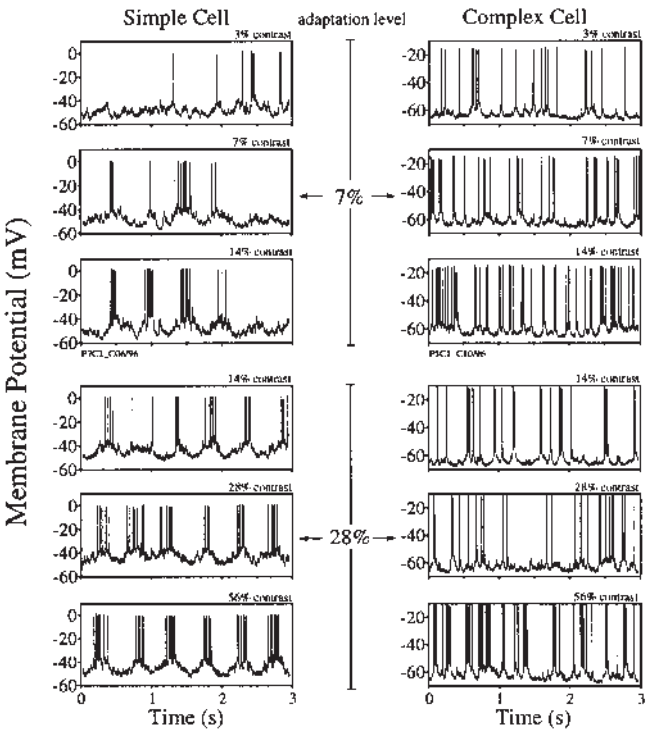

Figure 1. Intracellular records (3 s) from a simple cell (S3, OD group 7, directionally biased; records shown in the left column) and a complex cell (standard complex, OD group 1, and directionally biased; records in right column). The upper three records were obtained in a cell that had been pre-adapted for 10 s to a moving sinusoidal grating, optimized for spatial and temporal frequency, at a contrast level of 7%. The cell was then presented with the moving sinusoidal grating successively at contrasts of 3% (top records), 7% (middle records) and 14% (lower records) in a pseudo-random sequence. The lower three records were obtained by repeating the above sequence but at a pre-adapting contrast level of 28%, with test responses to contrast levels of 14, 28 and 56%. For the simple cell, the membrane potential underwent a periodic modulation but with no systematic shift in its mean level. For the complex cell, modulation of the membrane potential was not evident and nor was there any systematic shift in the mean level of the membrane potential with contrast. Spike height recorded for the complex cell increased for the 28% contrast adaptation protocol due to improved capacitance neutralization.

cyclic firing pattern as the sine wave grating passes over the receptive field (Movshon *et al.*, 1978a). For the complex cell, the modulations are not apparent and the cell responds with a much more irregular and bursty firing pattern than the simple cell. In the examples shown the neurons were adapted to two different contrast levels: 7 and 28%. For a given level of adaptation it is evident that response to the test stimulus increases with contrast. However, it is also evident, even from these single trials, that the state of adaptation strongly modifies the response. In particular, the responses to the 14% contrast should be compared, because these show the response of the cell to the same stimulus, but presented under two different states of adaptation. It is evident even from the single trials presented in Figure 1 that the responses of both the simple and the complex cell to the 14% contrast grating were higher when these neurons were adapted to a mean contrast of 7% than when they were adapted to 28%. This was also reflected in the average response of the neurons. For example, when adapted to 7% contrast gratings the simple cell responded to the 14% contrast grating with a mean firing frequency of 15 spikes/s, but the response was only 7 spikes/s when adapted to the 28% contrast grating.

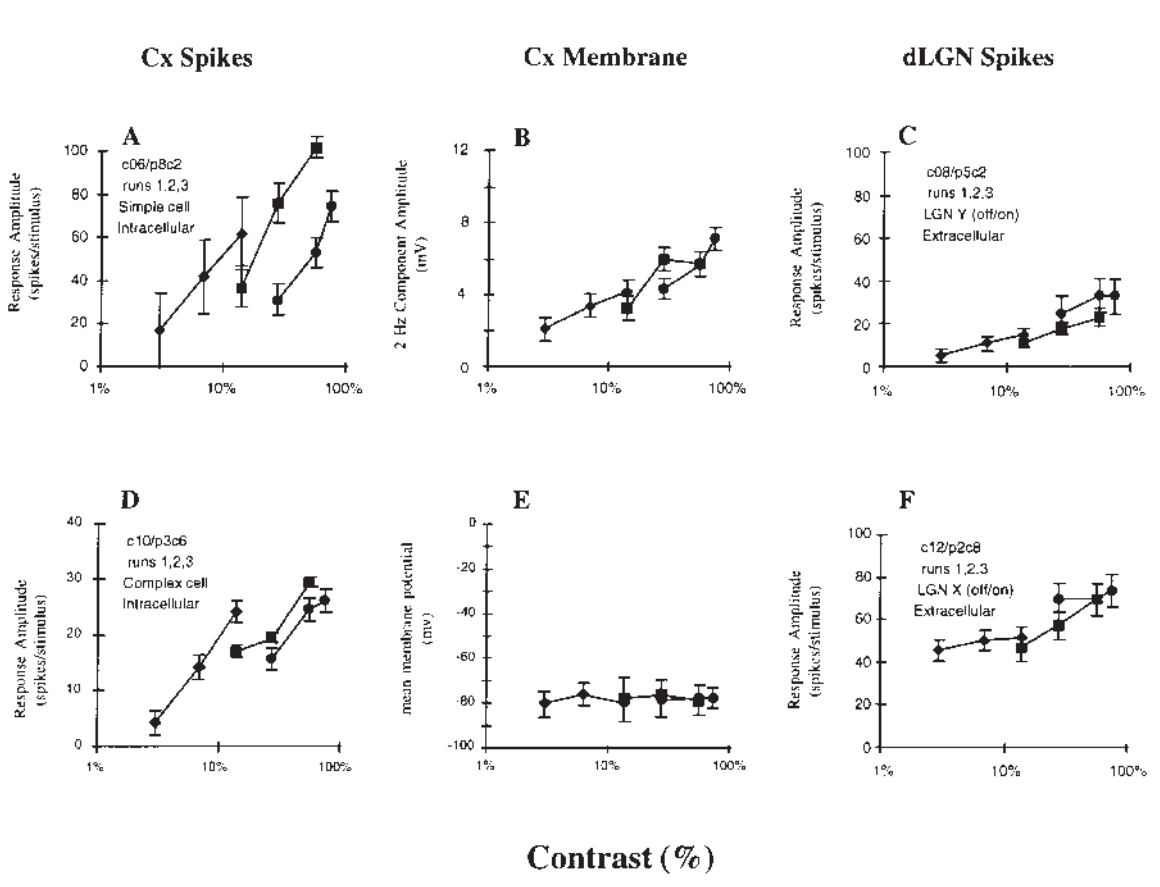

Figure 2. Response of visual cortical and dorsal lateral geniculate (dLGN) cells as a function of contrast. As the mean (i.e. adapting) contrast is increased from 7% (diamonds) to 28% (squares) to 56% (circles), the spike responses from an intracellularly recorded simple cell (*A*) and an intracellularly recorded complex cell (*D*) display the rightward shifts and response decrements characteristic of contrast adaptation. (*B*) The peak-to-peak amplitude of the 2 Hz component in the simple cell's membrane response to a 2 Hz stimulus exhibits no contrast adaptation. The amplitude of the dominant component (i.e. 2 Hz) increases monotonically with contrast regardless of the adaptation level. If fact, the response of the 2 Hz component more closely resembles the spike output recorded from dLGN neurons during identical experiments (*C* and *F*). (*E*) The mean membrane potential of the complex cell plotted as a function of contrast exhibits no change as the adapting contrast level is increased. The mean membrane potential remains unchanged across a broad range of stimulus contrasts.

The relationship between spike response and contrast for different levels of adaptation is plotted in Figure 2*A*,*D* for similar data derived from intracellular recordings from two other (one simple, one complex) cells. All three adapting levels were used and three levels of test contrast were applied for each (the highest test contrast in the case of the adaptation to 56% was 75%). The CRFs of both the simple cell (Fig. 2*A*) and the complex cell (Fig. 2*D*) show the typical steep slope for a particular level of adaptation. For increasing levels of adaptation, the CRF function shifts to a new average operating range. This is the dynamic process of contrast adaptation. Note that as the CRFs shift rightward on the log contrast axis, their slope remains approximately the same. This means that the gain of the CRF, defined as the ratio of magnitudes of response and stimulus, decreases with adaptation.

The data illustrated in Figure 2 indicate that similar results are obtained with intracellular recording as have been previously reported for extracellular recording (Ohzawa *et al.*, 1985; McLean and Palmer, 1996). Thus the impalement itself evidently does not interfere with the mechanisms that control the contrast gain function or adaptive shift of the CRF. However, the advantage of the intracellular recording is that it not only gives a direct view of the somatic membrane potential during the subthreshold events that lead to the generation of the action potential, but it also permits biophysical measurements to be made of the input conductance of a neuron under different states of adaptation.

The retinal signal is transmitted through the relay cells of the dorsal lateral geniculate nucleus (dLGN), which provide excitation to their cortical targets on each half of the sine wave cycle. The spike output of the simple cell similarly shows a pattern that approximates the half-wave rectified shape of the excitation. However, it is evident even in the single trial records of Figure 1 that the subthreshold membrane fluctuations approximate a full sine wave. This was confirmed by removing the spikes and performing a Fourier transform on the membrane potential. The dominant component in the frequency spectrum (not illustrated) was that of the stimulating grating. Thus, the membrane potential approximates a full sine wave, presumably because the excitatory signal transmitted from the dLGN rides on a maintained spontaneous discharge, which can be reduced by inhibition or increased by excitation. Active inhibition from the neurons that generate the antagonistic response in simple cell subfields drive the membrane potential more negative, as push–pull models of simple receptive fields describe (Palmer and Davis, 1981; Horton and Sherk, 1984; Ferster, 1986, 1988). The negative-going part of the sine wave stimulus is clearly reflected in the membrane potential of the simple cell shown in Figure 1.

If the membrane potential fluctuation reflects the underlying

dLGN signal with reasonable fidelity, then the amplitude of this membrane fluctuation should mimic the contrast-modulated signal arising from the dLGN. We established the profile of the dLGN relay cells contrast response by recording from three single dLGN fibres in the vicinity of the same cortical neurons, so as to match eccentricity, and then applied the same stimulus as was used for the cortical neurons. We then compared the responses of dLGN neurons with the amplitude of the membrane fluctuations, measured at the dominant component frequency of the sine wave stimulus. The results from one X cell and one Y cell are shown in Figure 2*C*,*F*. The spike output of the dLGN cells, was approximately monotonic with contrast whether they were X- or Y-type, as has been previously described by Ohzawa *et al.* (1985).

The component amplitude of the membrane potential of the simple cells all exhibited the behaviour shown in Figure 2, in which the response, like that of spike output of the dLGN relay cells, is approximately monotonic with contrast. The increase in the component amplitude response of the membrane potential from lowest contrast (3%) to highest (75%) is ~6 mV for this example. The two other simple cells showed increases of ~8 mV. Thus the whole dynamic range of the contrast signal, as reflected in the component amplitude, is compressed into a very narrow voltage range. Over the same range the dLGN spike rate increases by ~30 spikes/s. Of course in the case of the simple cell, the entire dynamic range is carried not only by the membrane potential, but also by the spike output. However, it is clear that when the spike output is compared with the membrane potential response, there is a mismatch: the spike output of the simple cell is only monotonic with contrast for a particular state of adaptation. As the state of adaptation shifts, so does the CRF. However, the component amplitude of the membrane potential shows no such adaptation and resembles much more the pattern seen for the dLGN relay cells' spike discharge.

The measurement of the component amplitude is, of course, complicated by the fact that a spike discharge occurs around the peak of the depolarizing phase of the sine wave. The spike discharge shunts some of the input current (Douglas *et al.*, 1994, 1996) and so attentuates the peak. However, comparison of the amplitude of the 2 Hz component of the membrane reponses at different contrasts (Fig. 2*B*) indicates that the component amplitude response has not saturated even at the highest contrast. Experiments from our laboratory *in vitro* (P. Goodman and K. Schindler, in preparation) and *in vivo* (B. Ahmed *et al.*, in preparation), using sine wave injections of current at different resting potentials, indicate that the maximum attenuation in the component membrane voltage fluctuation is only ~30% over a wide range of suprathreshold firing rates. Thus the lack of strong adaptation in the membrane voltage vs. contrast plot (Fig. 2*B*) is not explained solely by a compression artifact due to the existence of the spike threshold. The form of the curve may reflect the purely feedforward excitatory current provided by the dLGN afferents.

For complex cells, we cannot measure a single component amplitude of the response of the membrane potential to different contrasts during different states of adaptation. Nevertheless, after removal of the spikes, we can measure the mean membrane potential for the different contrast conditions. All four cells tested showed the pattern illustrated in Figure 2*E*, where there was little change in the mean membrane potential for the different test contrasts and for the different states of adaptation. In the example of the complex cell illustrated in Figure 1, when the neuron was adapted to a 7% contrast grating, it responded to a 14% contrast grating with a mean firing frequency of 15 spikes/s, but only 6 spikes/s when it had been adapted to a 28% contrast grating. The lack of shift in the mean membrane potential may indicate that for complex cells, the excitatory synaptic events arrive in temporally discrete packets that immediately drive the complex cell through threshold, rather than providing a continuous synaptic current whose amplitude is determined by the test contrast.

Clearly, for both simple and complex cells there is a transformation that takes place between the membrane potential and the spike output. It is this transform that determines both the shape of the CRF and the position of its operating point. In the Carandini and Heeger (1994) (C–H) model, the form of the CRF comes about by a shunting inhibitory mechanism which is driven by the activity of a pool of neurons. The C–H model predicts that the input conductance of a neuron increases dramatically over the full range of contrasts because the inhibitory shunt increases as a function of contrast. The presence of a shunting inhibition should be reflected by a measurable change in the input conductance of the cell. Ideally, the input conductance should be measured during exposure to different contrasts because the time constant of the conductance change has to be fast in this model.

Unfortunately, it is not technically possible to measure the conductance with conventional current pulses during the time the contrast response function is being measured because of the distortion in the measurements produced by the spike discharge. However, the presence of a large shunt can be detected indirectly in simple cells by measuring the peak-to-peak amplitude of their membrane deflections at different test contrasts. Because the input to the cortex from the dLGN relay cells is linear with contrast, large increases in the input conductance of the cortical neurons should be visible by a decrease in the magnitude of voltage deflection in simple cells produced by the test stimulus at different contrasts. The results of this measurement are illustrated in Figure 2*B*, which shows that the amplitude of the membrane potential deflection increases monotonically with contrast. Similar results were obtained from the other simple cells. Thus, for a given state of adaptation the input current to the neuron reflects the same form as the dLGN contrast response function.

Furthermore, we compared the responses of the three simple cells – both the spike discharge and the amplitude (peak-to-peak, measured for the frequency of the peak component in the Fourier transform) of their membrane fluctuations – for the same stimulus (14% contrast) presented under two different states of adaptation (7 vs 28%). The results for all three cells were consistent. The difference in the spike discharge rates were dramatic. For a 14% contrast grating, the response was reduced on average by 54% when the neurons were adapted to 28% compared with when they were adapted at 7% contrast. The comparable change in the amplitude of the membrane potential fluctuation was small by comparison – 12% – which amounts to <1 mV. These differences are illustrated qualitatively for the simple cell illustrated in Figure 1 and quantitatively for the simple cell illustrated in Figure 2. Thus the membrane shows little evidence of a strong shunt with this indirect measure. There is no evidence in these data that the input conductance of the neuron changes over the range of contrast tested.

Although the C–H model does not address the question of contrast adaptation, their idea could provide an explanation for the shift in the CRF due to prolonged exposure to a given

contrast. A shunting inhibitory mechanism that increased membrane conductance with increasing contrast would raise the synaptic current threshold for action potential production and decrease the gain of the CRF, which is what happens with contrast adaptation. Here the time constant of the adaptation process is 5–10 s, so the conventional conductance measurement methods of injecting a small 50 ms hyperpolarizing current pulse into the neuron and measuring the voltage deflection in the membrane potential near the end of the pulse could be applied. However, we have previously indicated that under *in vivo* recording conditions, such measurements have a limited accuracy (~20%) due to the spontaneous fluctuations in membrane potential and input conductance. This could be somewhat circumvented by undertaking a large number of trials. Unfortunately, large numbers of trials are rarely possible *in vivo* (Douglas *et al.*, 1988), so we used a limited number of current pulses. To reduce additional membrane noise in the present measurements we stopped the stimulus movement after each 3 s stimulus trial, displayed the mean contrast grating for a brief period (500 ms), and applied one test current pulse before resuming the stimulus movement. The magnitude of the pulse was varied quasi-randomly so that for each test contrast a number of values were obtained.

The voltage response to a hyperpolarizing pulse of 0.4 nA of 50 ms duration is shown for a single trial in Figure 3*A*. This was obtained from a neuron with an S-type (simple) receptive field that was adapted to a contrast level of 7%. Figure 3*B* shows the response to the same current step applied immediately after the moving grating (adapting contrast indicated) stopped. The adapting contrasts were 7, 28 and 56%, and 2–6 trials at each contrast were averaged. Although the data are relatively noisy, there was no consistent relationship between state of adaption to the various contrasts and the input conductance measured with the brief hyperpolarizing current pulse. The most consistent trend was found for the complex cell illustrated in Figure 1, but even here the result was not clear-cut. When the neuron was adapted to the 7 and 28% contrast levels there were small increases in the conductance as the neuron was stepped from lower to higher test contrasts. The increase in the conductances were small; for example, the change obtained for the lowest and highest test contrasts when the neuron was adapted to a contrast of 7% was of the order of 18%. However, there was no such consistent relationship between input conductance for this neuron and test contrast when it was adapted to a grating of 56% contrast.

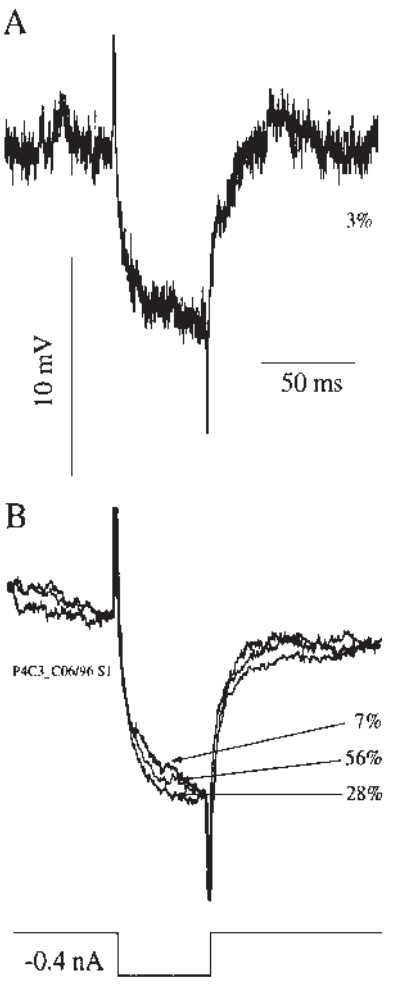

Figure 3. Records of intracellular responses to a current step of –0.4 nA (50 ms duration) for a simple cell (S1, OD group 1, and direction selective). (*A*) Single record obtained following presentation of a moving sinusoidal grating at a contrast level of 3%. (*B*) Shows three traces which have been filtered (to remove high frequency noise) for clarity of comparison. The cell was pre-adapted to a moving sinusoidal grating at a contrast level for 10 s, and then membrane voltage records were obtained 100 ms following 3 s presentations of stimulus grating during presentation of a stationary grating. The data are for pre-adaptation contrast levels of 7, 28 and 56%.

Discussion

The extensive extracellular analysis of the cortical mechanisms of contrast gain control and adaptation have indicated that there are two key mechanisms that remain unexplained. One is the enhanced gain of the contrast response function relative to that of the dLGN neurons. The other is the shift in the CRF when the neuron is exposed for 5–10 s to a different average contrast. Previous studies have indicated that the hyperbolic ratio function gives a satisfactory fit to most of the experimental data recorded from both cat and monkey (Albrecht and Hamilton, 1982; McLean and Palmer, 1996). However, the underlying circuits and physiological processes that produce the characteristic shape and adaptive shifts of the CRF remain a subject for discussion. Bonds (1991, 1993), for example, has suggested that the CRF may not be the product of a single process and thus fitting with a single function may be incorrect. The C–H model is the most elegant and biological in its conception to date and thus is an obvious focus for experimental testing. Although normalization for contrast does appear unbidden and unexplained in the 'emergent model' developed by Somers *et al.* (1995), contrast adaptation does not. Thus we still seek some coherent framework within which contrast gain control and contrast adaptation can be understood at the level of known cortical circuits.

To take another step in this important analysis we have employed the technique of intracellular recording and have used the visual stimulation protocols used in extracellular studies of contrast gain control and adaptation. The intracellular recording technique supplies us with a view of subthreshold events that give us further significant clues to the underlying mechanisms and also offers the possibility of tying these phenomena down to some aspects of the structure of the cortical circuits. With this technique we were able to record intracellularly from both simple cells and complex cells (S-type and C-type fields respectively), and make some measurements of the amplitudes of the membrane fluctuations in the case of the simple cell

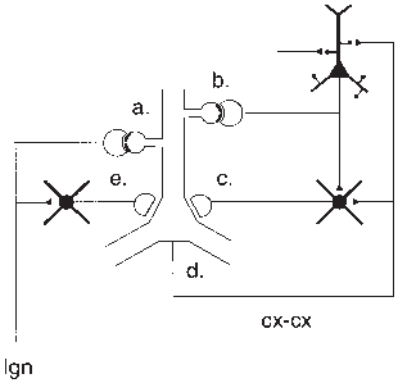

Figure 4. Schematic of geniculo-cortical and cortico-cortical connections that could contribute to the contrast gain properties of cortical neurons. The large open shape represents a typical spiny neuron of cortex, receiving excitatory asymmetric synapses (a, b) from geniculate relay cells and other intracortical spiny neurons; as well as inhibitory symmetrical synapses (e, c) from cortical smooth neurons. In the light of this circuit, contrast gain control and adaptation could occur by (i) adaptation of excitatory synapses or dendritic gain (a, b); (ii) modification of recurrent excitation (b); (iii) 'normalizing' feedback shunting inhibition (c); (iv) adaptation of neuronal action potential generation (d); or (v) 'normalizing' feedforward inhibition (e).

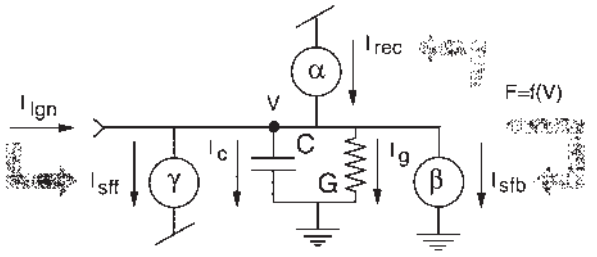

Figure 5. Basic electrical model used to discuss contrast gain in this paper (see text). Circles indicate current sources. *G*, neuronal input conductance; *C*, neuronal capacitance; α, network conductance arising out of recurrent connections with other cortical spiny cells; β, network conductance arising out of recurrent connections with other smooth spiny cells; γ, coupling co-efficient between geniculate afferent activity and feedforward inhibition; I_{lgn}, feedforward geniculate input; I_g, leak current; I_c, capacitative current; I_{rec}, feedback recurrent excitatory current from intracortical spiny neurons; I_{sfb}, feedback recurrent inhibitory current from intracortical smooth cells; I_{sff}, feedforward inhibitory current from intracortical smooth cells driven by geniculate afferents. Grey 'information' arrows indicate coupling between discharge rates and relevant neuronal currents. Discharge rate of this basic neuron is a linear-threshold function of capacitor voltage, *V*.

responses and measure the action potential discharge. Importantly, the impalement itself did not alter the expression of the basic phenomenon. Thus, whatever the perturbation made by the impalement, we can be confident that the subthreshold phenomena must reliably reflect the normal voltage fluctuations that lead to action potential discharge.

In the intracellular recordings made here we were able to provide evidence that there are no large changes in the input conductance of neurons when exposed to test stimuli of different contrast for a short duration. This observation is counter to the prediction made by Carandini and Heeger (1994), who predicted that the conductance of a simple cell should increase by ~4-fold when exposed to a full contrast grating. We could not stimulate with a full contrast grating, but even over a substantial range of contrast, e.g. 14–56% we were unable to detect the marked change in the amplitude of the stimulus-induced membrane fluctuations that should have been obvious had a shunting inhibition been present. Although the test we used was indirect because of the technical limitations of measuring conductance changes in an active neuron *in vivo*, the appearance of a strong shunt would have been remarkable in the face of evidence that every other aspect of visually evoked inhibition in the visual cortex *in vivo* that has been studied to date has not involved a large shunting mechanism. Thus, the solution offered by the model of Carandini and Heeger (1994) is not supported by our data. This unfortunately leaves us short of a clear explanation for the saturation that contributes to the hyperbolic form of the CRF.

In the case of contrast adaptation, extracellular recording studies have not revealed the mechanism by which the operating point is adjusted. There seems to be general agreement that no drugs yet applied to agonize or antagonize various excitatory or inhibitory transmitter receptors have had a marked effect on contrast adaptation (DeBruyn and Bonds, 1986; Vidyasagar, 1990; McLean and Palmer, 1996). McLean and Palmer (1996) found a slight effect on the CRF when they blocked presynaptic metabotropic glutamate receptors, but contrast adaptation still was marked even when these receptors were blocked. Activating the presynaptic metabotropic glutamate receptors might have been a more effective test in this instance. On the basis of these studies it seems that the answer to adaptation is not to be found in synapses. Nevertheless, most workers continue to favour an inhibitory-type mechanism to explain contrast adaptation, especially because the alternative possibility that the effect is caused by fatigue of the neuron under study has also been ruled out (Ohzawa *et al.*, 1985; DeBruyn and Bonds, 1986; Geisler and Albrecht, 1992). Indeed, we have driven neurons by direct injection of depolarizing currents and sine wave currents into the neuron for lengthy periods (up to 30s) and have found that the spike adaptation mechanisms cannot account for the marked changes in responsiveness seen during contrast adaptation (B. Ahmed *et al.*, in preparation).

It has been suggested (Vidyasagar, 1990) that the mechanism of contrast adaptation is a cooperative one that involves many more neurons than those affected by the iontophoretic application of drugs. However, as yet there has been no more formal explanation of how contrast adaptation might be achieved within the known circuits of the cat visual cortex. Here we explore whether the model of recurrent circuits we have used to explain other aspects of visual processing (Douglas and Martin, 1991; Douglas *et al.*, 1995, 1996) might not provide a means of explaining the intracellular data we have gathered here for contrast gain control and contrast adaptation.

Electronic Equivalent Circuit for Recurrently Connected Neurons

In this section we will discuss the response of cortical simple cells to contrast in the context of the simplified neuron circuit shown in Figures 4 and 5. This circuit provides a convenient heuristic for interpreting some key features of our results. Obviously, such a simple model is not intended to provide a comprehensive account of all details of the physiological data, but even in this simple form it does capture critical features of the experimental results. The neuronal circuit is interpreted as an electronic model that represents the geniculo-cortical and cortico-cortical effects on a typical cortical excitatory neuron embedded in the neuronal circuit shown in Figure 5. With one addition, it is of the same basic form as that we have previously used and justified on grounds of detailed anatomy and physiology (Douglas *et al.*, 1995, 1996). A feedforward inhibitory pathway, represented by the current source γ in the

schematic has been added to the previous model. There is substantial anatomical and physiological justification for this additional direct pathway (Freund *et al.*, 1985b; Douglas *et al.*, 1989, 1991; Ahmed *et al.*, 1997). In addition, there may be a polysynaptic feedforward excitatory and inhibitory pathway involving layer 6 pyramidal cells, some of which are themselves directly excited by dLGN afferents and form synapses with spiny and smooth neurons in layer 4 (Martin and Whitteridge, 1984; McGuire *et al.*, 1984; Ahmed *et al.*, 1994, 1997). We have included feedforward inhibitory pathways in previous anatomical circuit diagrams, but have not explored their properties and potential in the electronic model. The details of the operation of the recurrent inhibitory and excitatory circuits have been dealt with in some detail elsewhere (Douglas *et al.*, 1995, 1996) and will not be rehearsed in the description of the model given below.

Briefly, the excitatory (pyramidal or spiny stellate) neuron is represented as a conductance, G, and capacitance, C (Fig. 5). The resting state of the transmembrane potential is at ground potential (V_m = 0). The output discharge frequency of the 'neuron' is represented by a continuous variable, F, which is a linear-threshold function of V_m. We usually choose this function to have a discharge threshold of a few millivolts, and to provide ~70 events/s (equivalent to spikes/s in real neurons) for 1 nA input current into G = 50 nS. The synaptic inputs to the model neuron are modelled as current inputs (and so depicted as current sources in Fig. 5). The neuron receives excitatory current from two pathways: a feedforward input, I_{lgn}, which represents the dLGN afferent input to layer 4; and a feedback input, I_{rec}, which represents the input received from intracortical recurrent excitatory circuits (Douglas *et al.*, 1995, 1996). Inhibitory current also arises from two pathways: a feedforward input, I_{ff}, which expresses the effect of smooth cells in layer 4 driven by the dLGN input to layer 4; and a feedback input, I_{fb}, which represents the input received from intracortical recurrent inhibitory circuits (Douglas *et al.*, 1995, 1996).

In this basic model all the recurrent excitatory neurons are considered to be identical and they are represented as a single lumped excitatory synapse. The effect of this lumped synapse is approximated as a current source (labelled α in Fig. 5). The current delivered by the source is proportional to the average firing rate of the neurons within a recurrently connected population (indicated by the grey 'information' arrow). All the members of the population receive similar inputs and have similar connectivity, so the average firing rate for the population is also the discharge rate of the particular neuron described here. But the firing rate depends on the voltage, V, of the neuron. This means that the recurrent current received by a neuron within the population is proportional to its own voltage, $I_{rec} = \alpha V$. Thus, recurrent excitation generates an effective 'network conductance' α. In the case of recurrent excitation the network conductance is negative, and so the effective input conductance, G_{eff}, of the neuron becomes smaller than its physical value, G. A similar argument obtains for recurrent inhibition, except that its network conductance, β, is positive and so adds to the effective input conductance of the neuron.

In addition to recurrent inhibition, we have included also a feedforward inhibition that is proportional to geniculocortical excitation. This inhibition provides feedforward scaling of the input signal as indicated by the grey 'information' arrow at the left of Figure 5. The feedforward inhibitory current, I_{sff}, is proportional, by γ, to the geniculocortical activation. We treat inhibition as linear hyperpolarizing currents, neglecting the shunting aspects of inhibitory inputs, since significant shunts have not been observed experimentally *in vivo* (Douglas *et al.*, 1988; Ferster, 1988; Berman *et al.*, 1989; Douglas and Martin, 1989; Pei *et al.*, 1991). With the inhibitory circuit added, the effective conductance of the neuron, G_{eff}, is the sum of the individual neuron conductance G, and the two network conductances, α for the excitatory circuit and β for the inhibitory circuit. The effective conductance of the neuron is given by $G - \alpha + \beta$. The magnitude of the recurrent inhibitory current is βF and the total recurrent current arriving at the soma is given by $I_{rec} = (\alpha - \beta)F$; the output firing frequency of the neuron, F, is $(I_{lgn} - I_{sff})/(G + \beta - \alpha)$.

The important point made by this simple model is that recurrent connections between a population of cortical neurons can modify the effective input conductances of the participating neurons so that they individually amplify (or attenuate) the geniculocortical input current. The degree of amplification has yet been determined experimentally, but estimates based on existing anatomical and biophysical data suggest that factors of up to ~5 can be expected (Douglas *et al.*, 1995). The properties of this simple model can be expressed also in more detailed, biophysically realistic simulations (Douglas *et al.*, 1995; Suarez *et al.*, 1995).

It is important to note that although the synapses themselves are 'linear' or 'subtractive', the change in the *F–I* curve during recurrent inhibition is not, as one might expect, a simple rightward shift in the curve. Instead, the slope decreases, as if the excitatory current is being shunted or divided. This divisive process occurs here because the inhibition applied is proportional to the output of the neuron (see Douglas *et al.*, 1995, 1996). It is widely assumed, following Blomfield (1974), that shunting inhibitory synapses acting on the somata of single neurons produce a divisive change in the current–discharge relationship. In fact, experiment and theory show that they do not (Connors *et al.*, 1988; Douglas and Martin, 1990; Berman *et al.*, 1992; Holt and Koch, 1997). However, our model explains how 'division' can occur in networks: feedback inhibition, acting through approximately linear 'subtractive' synapses, generates a network conductance that appears as a divisive change in the spike discharge rate of the neuron. This inhibition changes the gain of the cortical response to a given input current and it explains how inhibition of the spike discharge of the neuron appears divisive (Rose, 1977; Morrone *et al.*, 1982b; Dean *et al.*, 1980) when intracellular recordings clearly indicate that the shunts associated with inhibitory events are extremely modest (Douglas *et al.*, 1988; Berman *et al.*, 1991; Ferster, 1988; Pei *et al.*, 1991) and largely induce small amplitude hyperpolarizations.

Contrast Response of Cortical Neurons

The model shown in Figure 5 was driven by an input signal, I_{lgn}, derived as the product of a 1 Hz sinusoidally modulated contrast stimulus, the geniculate contrast response function (Fig. 6, trace *A*, and geniculo-cortical synaptic efficacy assumed to be 0.5 nA somatic current at 100 events/s synaptic excitation, or 0.005 pC/event). The CRF function of the dLGN relay cells was taken to be $(110 \times c)/(0.4 + c)$, which is representative of measurements for cat dLGN (Sclar *et al.*, 1990).

Our direct intracellular measurements from cortical simple cells showed that the subthreshold membrane potential is approximately sinusoidally modulated by sinusoidal contrast stimuli and is not half-wave rectified. This observation suggests

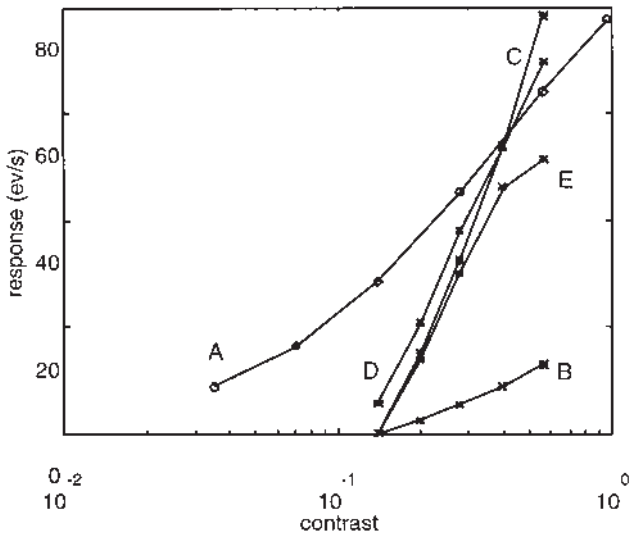

Figure 6. Contrast response functions of a lateral geniculate neuron (*A*) and various models of cortical neuron (*B–E*). (*A*) Typical geniculate response, obtained from the Naka–Rushton relation with a semisaturation contrast of 0.4, and an exponent of 1 (Ohzawa *et al.*, 1985). The cortical responses were obtained from various versions of the model neuron shown in Figure 5. (*B*) Cortical neuron with small feedforward input only has low gain over the range of contrasts tested. (*C*) High gain response obtained by increasing current discharge relation by a factor of 6. (*D*) High gain response obtained by increasing the feedforward current by a factor of 6 (with respect to *B*). (*E*) High gain response obtained by recurrent excitation. Feedforward current is the same as in *B*.

that each cortical simple cell receives both ON and OFF input from the LGN, presumably via a push–pull interaction of excitation and inhibition (Palmer and Davis, 1981; Horton and Sherk, 1984; Ferster, 1986, 1988; Carandini and Heeger, 1994). Therefore, both the positive and negative components of I_{lgn} were used as input to our model. Of course, this leads to a sinusoidal modulation of membrane potential of the model cortical neuron, and the amplitude of this modulation grows approximately linearly with log contrast, as observed in the real neurons (compare Fig. 6).

The adapted current–discharge relation of cortical neurons is ~70 events/s/nA when measured *in vitro* or *in vivo* (B. Ahmed *et al.*, unpublished data). Since the modulation of the input current was slow by comparison with typical discharge adaptation time constants (~20 ms), the adapted current discharge relation can be used to estimate the output discharge of the model cortical neuron. The resulting prediction of the cortical CRF for a purely feedforward model is shown in Figure 6. The CRF is quite flat, and does not show the high gain found in the mid-range of a given CRF, which is fits well the steep slope of the linear portion of the Naka–Rushton function. For example, typical experimentally observed CRFs have a slope of ~100 spikes/s per decade of contrast, whereas the response of the feedforward model in Figure 6 (trace *B*) has a slope of only 20 events/s. The question is, where is the additional gain obtained? There are several possibilities.

One possibility is that the current–discharge relation of cortical neurons is actually much higher than used in the model, e.g. 400 rather than the typical 70 events/s/nA (Fig. 6, trace *C*). This change certainly improves the maximum gain, but is way out of range of the *F–I* relations measured experimentally. We have made direct measurements of the adapted *F–I* relations in the same cells from which discharge CRFs were obtained intracellularly. The average slope was 71 spikes/s/nA (SEM 8.6 spikes/s/nA, $n = 10$).

A second possibility is that the input current received by the neuron is much greater than that modelled. For example, a dense anatomical convergence of the dLGN afferents coupled with very strong synapses could be a source of exceptionally large currents in single simple cells. In the feedforward case, this means that I_{lgn} must be larger than modelled by a factor of ~4–5 (Fig. 6, trace *D*). This solution seems unlikely, given that only ~5% of excitatory synapses onto the input cells of cortex are provided by the dLGN afferents (Ahmed *et al.*, 1994), and the dLGN synapses, while exceptional in having a high probability of transmitter release, do not produce EPSPs that are an order of magnitude larger than those of other cortical cells in layer 4, for example (Stratford *et al.*, 1996). In addition, the model needs to be applicable to neurons in other layers, where the primary input is from conventional cortical synapses (Mason *et al.*, 1991; Thomson and Deuchars, 1994). Thus having a 'special purpose' geniculocortical synapse that supplies a large feedforward input current does not solve the problem.

In the feedback case, the recurrent currents provide a large fraction of the total somatic current and the amplitude of I_{lgn} is relatively small. The dLGN current input is simply amplified by summation with I_{rec}. This recurrent gain can provide the necessary increase in slope (Fig. 6, trace *E*). The *F–I* response of the linear threshold neurons used in the model is also linear. Consequently, the linear response of the cortical neurons to log contrast is derived from the log contrast behavior of the dLGN input.

Contrast Adaptation

In real cortical neurons the CRF adapts in relation to the average contrast of the stimulus (Figure 2), with a time constant of ~5–10 s (Albrecht *et al.*, 1984; Ohzawa *et al.*, 1985; Bonds, 1991). There are a number of mechanisms that could underly this adaptation (Fig. 4*A*). For example, the efficacy of excitatory synapses (or perhaps dendritic gain) could adapt in response to sustained high input signals (Markram and Tsodyks, 1996; Abbott *et al.*, 1997). The reduction in the neuronal discharge seen during adaptation would then be due to a reduction in the amplitude of the sinusoidal driving signal at the soma or the action potential initiation zone. We found no such changes in amplitude during contrast adaptation in our direct intracellular measurements (Fig. 2).

An alternative possibility is that the sensitivity of the neuron is reduced by shunting inhibition. But this divisive mechanism too should express itself as an adaptation-dependent reduction in the stimulus induced membrane fluctuations. A third possibility is that the spike generation mechanism undergoes long time-constant adaptation during sustained discharge. Although some quite long time-constant outward conductances have been observed in cortical neurons (Schwindt *et al.*, 1988a,b), the strength of those currents is not enough to provide the ~0.5 nA outward current to achieve the degree of reduction in discharge observed in Figures 1 and 2*A*, for example. Indeed, activity itself has no effect on the process of contrast adaptation, since decreases or increases in the discharge rate induced by drugs during the visual adaptation period do not alter contrast adaptation (DeBruyn and Bonds, 1986; Vidyasagar, 1990; McLean and Palmer, 1996; J. Allison and K. Martin, in preparation).

A further possibility is that the contrast adaptation is due to feedforward inhibition that is proportional to average geniculate

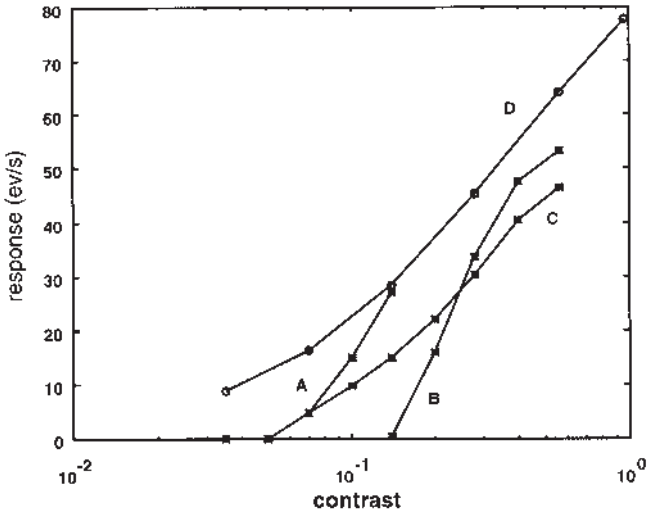

Figure 7. Adaptation of action potential contrast response in model cortical neuron by normalizing feedforward inhibition derived from time averaged (time constant, 10s) geniculate input signal. (*A*) Transient contrast response function (CRF) of model cortical neuron shown in Figure5 measured at an adapting contrast of 0.07. This CRF estimates the differential mode CRF at the adapting contrast. (*B*) Transient contrast response function of model neuron measured at an adapting contrast of 0.28. (*C*) Slow CRFs measured at adapting contrasts of 0.07 and 0.28, estimating the common mode cortical CRF. This 'DC' response is similar to *D*, the geniculate CRF (*A* in Fig.6).

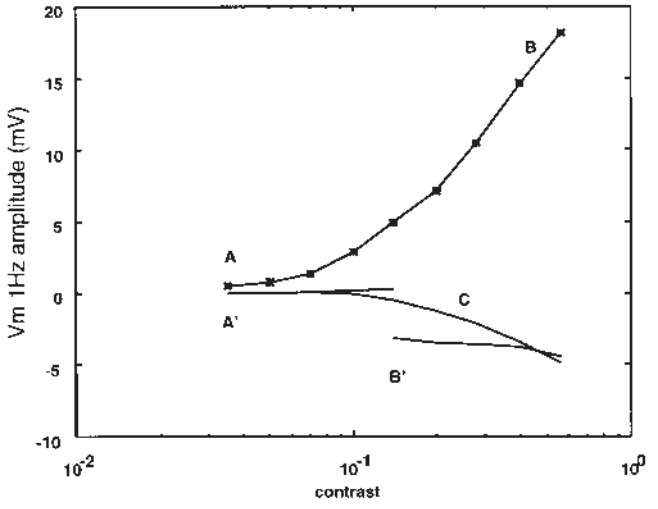

Figure 8. Membrane potential responses of the model cortical neuron. Amplitude of the 1Hz component, *A*, and average *A'* of the membrane potential response to a 1Hz sinusoidally modulated contrast stimulus when the neuron was adapted to a contrast of 0.07. These curves correspond to discharge responses *A* in Figure7. Curves *A* and *B* overlap for contrast of 0.14. (*B*) As *A*, but for contrast adaptation of 0.28. (*C*) Average membrane potential obtained when estimating the 'DC' CRF in *C* of Figure7. The amplitudes of the 1Hz component were superimposed on curves *A* and *B* above, and so are not plotted.

activity (γ in Fig. 5), with a time-constant of a few seconds. Such feedforward scaling would act by shifting the threshold of activation of the cortical neuron along the log contrast axis. The feedforward geniculate signal that provides excitation and inhibition (indirectly via an interneuron) to the cortical neurons is approximately linear in log contrast (Fig. 6, trace *A*). Therefore subtraction of these two signals is expected to result in a divisive shift, rightwards along the log contrast axis (Fig. 7). The subtractive inhibition should lead to a hyperpolarizing shift in the membrane potential.

If activation of the cortical neuron was purely feedforward, then the inhibitory current would have to be some substantial fraction of the excitatory current, and the resultant hyperpolarization should be large. For example, if the total excitatory current is ~1 nA, then to shift the CRF adapted at 7% contrast to the CRF adapted at 28% contrast would require a subtractive current of ~0.5 nA. This would produce a hyperpolarizing shift of ~10 mV for neurons of input resistances of ~20 MΩ. We did not observe such large hyperpolarizations. However, the mechanism of an inhibitory offset is theoretically interesting and the absence of mean membrane potential changes in our data can be readily explained if the input current to the neurons is amplified by the recurrent circuits (Fig. 5*B*). Under the conditions operating in the electronic model circuit, the effect of the inhibitory current is enhanced by the recurrence, because it is the interaction between the small feedforward excitatory current and the equally small feedforward inhibitory current that is amplified to provide the observed discharge response. The hyperpolarizing shifts caused by such inhibitory currents are expected to be small (2–3 mV in traces *A'* and *B'* of Fig. 8). Such small changes would be difficult to detect *in vivo*, where the mean membrane potential is somewhat dependent on the strength of activation of the neuron. We have not obtained convincing evidence for a consistent contrast-dependent shift in the average membrane potential of either simple or complex cells. However, we note that Carrandini and Ferster (1997) used a different protocol to ours and reported contrast-dependent changes in mean membrane potential of the order of 2–15 mV. If mean membrane potential changes of this magnitude underlie contrast adaptation they should have readily been detected with the stimulation protocol we used, but such large changes in membrane potential were not observed. It will be interesting to see whether the small changes predicted by our model might not be more readily revealed by another stimulation protocol.

Conclusion

We have used a simple, rather linear model to discuss the central features of our results. We have been concerned to emphasize the possible role of recurrent connectivity in the generation of the cortical CRF, and its possible modification by simple feedforward controls. That the model can capture some of the basic phenomena also indicates that mechanisms may be essentially local and not require long distance lateral interactions. The experimental work of Ohzawa *et al.* (1985) indicates that adaptation and gain control is indeed essentially a local phenomenon and can act within the receptive field itself.

Clearly, such a model will not provide a comprehensive account of all aspects of the problem. For example, we have not addressed the problem of the exact form of the CRF in cortex, in particular its saturation at discharge levels less than typical saturation levels of the individual neuronal *F–I* relation. Carandini and Heeger (1994) have suggested that this saturation arises from a shunting feedback inhibition that acts to normalize the cortical responses to changes in contrast. But the increases in conductance expected on the basis of their theory are not observed experimentally. It is possible that the saturation effects arise, for example, out of the interaction of recurrent excitation with dendritic saturation effects. We have also not identified the source of the relatively long time constant (6–10 s) of the contrast adaptation. The difficulty here, of course, is that studying possible candidates, e.g. modulation of synaptic

efficacy, is particularly difficult *in vivo* and the plethora of dynamic changes in synaptic efficacy seen *in vitro* (Thomson and Deuchars, 1994; Markram and Tsodyks, 199; Stratford *et al.*, 1996) remain to be demonstrated *in vivo*.

Another aspect that needs resolution is the role of inhibition in the adaptation response. Here we have explored how a feedforward inhibitory pathway might act to produce the contrast adaptation. However, experiments that have blocked the GABAa receptors locally with *n*-methyl bicuculline have failed to find evidence of a GABA-mediated inhibition. Clearly there are other inhibitory receptors in cortex, the $GABA_b$ receptor, for example (Connors *et al.*, 1988; Douglas *et al.*, 1989; Berman *et al.*, 1991). Their role needs now to be examined. Although most cortical neurons tested show contrast gain control and contrast adaptation, the strength of the effect varies greatly between neurons (Albrecht *et al.*, 1984; Ohzawa *et al.*, 1985). This aspect has yet to be understood. It is possible that the absolute contrast signal transmitted from the dLGN might be preserved in some neurons that participate in some particular pathways. Another possibility is that gain control and adaptation is done once only at the input stage and then transmitted within the cortical column to output neurons, much like the retina does with luminance. Whatever the answer to these and other important questions, it is clear that the mechanisms involved in the control of contrast have already provided and important extension to our exploration of the microcircuits of the visual cortex.

Notes

The preparation of this article was supported by the Swiss National Science Foundation SPP Grant, the Human Frontiers Science Programme and the US Office of Naval Research. We thank our colleagues for their encouragement and assistance.

References

Abbott L, Varela J, Sen K, Nelson S (1997) Synaptic depression and cortical gain control. Science 275:220–224.

Ahmed B, Anderson J, Douglas R, Martin K, Nelson C (1994) Polyneuronal innervation of spiny stellate neurons in cat visual cortex. J Comp Neurol 341:39–49.

Ahmed B, Anderson J, Martin K, Nelson J (1997) A map of the synapses onto layer 4 basket cells of the primary visual cortex of the cat. J Comp Neurol 379:1–13.

Albrecht D, Hamilton D (1982) Striate cortex of monkey and cat: contrast response function. J Neurophysiol 48:217–237.

Albrecht D, Farrar S, Hamilton D (1984) Spatial contrast adaptation characteristics of neurones recorded in the cat's visual cortex. J Physiol (Lond) 347:713–739.

Allison J, Ahmed B, Anderson J, Douglas R, Martin K (1996) Contrast gain control in neurons of the cat primary visual cortex: input–output analysis. Soc Neurosci Abstr 22:1705.

Berman N, Douglas R, Martin K (1992) Gaba-mediated inhibition in the neural networks of visual cortex. Progr Brain Res 90:443–476.

Berman N, Douglas R, Martin K, Whitteridge D (1991) Mechanisms of inhibition in cat visual cortex. J Physiol (Lond) 440:697–722.

Blomfield S (1974) Arithmetical operations performed by nerve cells. Brain Res 69:1115–1124.

Bonds A (1991) Temporal dynamics of contrast gain in single cells of the cat striate cortex. Vis Neurosci 6:239–255.

Bonds A (1993) The encoding of cortical contrast gain control. In: Contrast sensitivity (Shapley R, Lam D, eds), pp 215–230. Cambridge, MA: MIT.

Carandini M, Ferster D (1997) A tonic hyperpolarization underlying contrast adaptation in cat visual cortex. Science 276:949–952.

Carandini M, Heeger D (1994) Summation and division by neurons in primate visual cortex. Science 264:1333–1336.

Connors B, Malenka R, Silva L (1988) Two inhibitory postsynaptic potentials, and GABAa, and GABAb receptor-mediated responses in neocortex of rat and cat. J Physiol (Lond) 406:443–468.

Das A (1996) Orientation in visual cortex: a simple mechanism emerges. Neuron 16:477–480.

Dean A, Hess R, Tolhurst D (1980) Divisive inhibition involved in direction selectivity. J Physiol (Lond) 308:84–85P.

DeBruyn E, Bonds A (1986) Contrast adaptation in the cat visual cortex is not mediated by gaba. Brain Res 383:339–342.

Douglas R, Martin K (1990) Control of neuronal output by inhibition at the axon initial segment. Neural Computat 2:283–292.

Douglas R, Martin K (1991) A functional microcircuit for cat visual cortex. J Physiol (Lond) 440:735–769.

Douglas R, Martin K, Whitteridge D (1988) Selective responses of visual cortical cells do not depend on shunting inhibition. Nature 332:642–644.

Douglas R, Martin K, Whitteridge D (1989) A canonical microcircuit for neocortex. Neural Computat 1:480–488.

Douglas R, Martin K, Whitteridge D (1991) An intracellular analysis of the visual responses of neurones in cat visual cortex. J Physiol (Lond) 440:659–696.

Douglas R, Koch C, Mahowald M, Martin K, Suarez H (1995) Recurrent excitation in neocortical circuits. Science 269:981–985.

Douglas R, Mahowald M, Martin K (1994) Hybrid analog–digital architectures for neuromorphic systems. In IEEE International Conference on Neural Networks, Orlando, pp 1848–1853.

Douglas R, Mahowald M, Martin K, Stratford K (1996) The role of synapses in cortical computation. J Neurocytol 25:893–911.

Ferster D (1986) Orientation selectivity of synaptic potentials in neurons of cat primary visual cortex. J Neurosci 6:1284 1301.

Ferster D (1988) Spatially opponent excitation and inhibition in simple cells of the cat visual cortex. J Neurosci 8:1172–1180.

Ferster D, Jagadeesh B (1992) EPSP–IPSP interactions in cat visual cortex studied with in vivo whole-cell patch recording. J Neurosci 12:1262–1274.

Freund T, Martin K, Somogyi P, Whitteridge D (1985) Innervation of cat visual areas 17 and 18 by physiologically identified X- and Y-type thalamic afferents. II. Identification of postsynaptic targets by GABA immunocytochemistry and Golgi impregnation. J Comp Neurol 242:275–291.

Geisler W, Albrecht D (1992) Cortical neurons: isolation of contrast gain control. Vision Res 32:1409–1410.

Holt G, Koch C (1997) Shunting inhibition does not have a divisive effect on firing rates. Neural Computat (in press).

Horton J, Sherk H (1984) Receptive field properties in the cat's lateral geniculate nucleus in the absence of on-center retinal input. J Neurosci 4:374–380.

Hubel D, Wiesel T (1962) Receptive fields, binocular interaction and functional architecture in the cat's visual cortex. J Physiol (Lond) 160:106–154.

Livingstone M, Hubel D (1988) Segregation of form, color, movement, and depth: anatomy, physiology, and perception. Science 240:740–749.

Maex R, Orban C (1996) A model circuit of spiking neurons generating directional selectivity in simple cells. J Neurophysiol 75:1515–1545.

Markram H, Tsodyks M (1996) Redistribution of synaptic efficacy between cortical pyramidal neurons. Nature 382:807–810.

Martin K (1988) The Wellcome Prize Lecture: from single cells to simple circuits in the cerebral cortex. Quart J Exp Physiol 73:637–702.

Martin K (1994) A brief history of the 'Feature Detector'. Cereb Cortex 4:1–7.

Martin K, Whitteridge D (1984) Form, function and intracortical projection of spiny neurones in the striate visual cortex of the cat. J Physiol (Lond) 353:463–504.

Mason A, Nicoll A, Stratford K (1991) Synaptic transmission between individual pyramidal neurons of the rat visual cortex in vitro. J Neurosci 11:72–84.

McGuire B, Hornung J-P, Gilbert C, Wiesel T (1984) Patterns of synaptic input to layer 4 of cat striate cortex. J Neurosci 4:3021–3033.

McLean J, Palmer L (1996) Contrast adaptation and excitatory amino acid receptors in cat striate cortex. Vis Neurosci 13:1069–1087.

Morrone M, Burr D, Maffei L (1982) Functional implications of cross-orientation inhibition of cortical visual cells. i. Neurophysiological evidence. Proc R Soc Lond B 216:335–354.

Movshon J, Thompson I, Tolhurst D (1978) Spatial summation in the receptive fields of simple cells in the cat's striate cortex. J Physiol (Lond) 283:53–77.

Naka K, Rushton W (1966) S-potentials from colour units in the retina of fish (Cyprinidae). J Physiol (Lond) 185:536–555.
Ohzawa I, Sclar G, Freeman R (1982) Contrast gain control in the cat visual cortex. Nature 298:266–268.
Ohzawa I, Sclar G, Freeman R (1985) Contrast gain control in the cat's visual system. J Neurophysiol 54:651–667.
Palmer L, Davis T (1981) Receptive-field structure in cat striate cortex. J Neurophysiol 46:260–276.
Pei X, Volgushev M, Vidyasagar T, Creutzfeldt O (1991) Whole cell recording and conductance measurements in cat visual cortex *in vivo*. Neurosci Rep 2:485–488.
Rose D (1977) On the arithmetical operation performed by inhibitory synapses onto the neuronal soma. Exp Brain Res 28:221–223.
Schwindt P, Spain W, Foehring R, Chubb M, Crill W (1988a) Slow conductances in neurons from cat sensorimotor cortex *in vitro* and their role in slow excitability changes. J Neurophysiol 59:450–467.
Schwindt P, Spain W, Foehring R, Chubb M, Crill W (1988b) Multiple potassium conductances and their functions in neurons from cat sensorimotor cortex *in vitro*. J Neurophysiol 59:424–449.
Sclar G, Freeman R (1982) Orientation selectivity in the cat's striate cortex is invariant with stimulus contrast. Exp Brain Res 46:457–461.
Sclar G, Maunsell JR, Lennie P (1990) Coding of image contrast in central visual pathways of the macaque monkey. Vision Res 30:1–10.
Shapley R, Enroth-Cugell C (1984) Progress in retinal research. In: Visual adaptation and retinal cain controls (Osborne N, Chader O, eds), Vol 3, pp 263–346. Oxford: Pergamon Press.
Shapley R, Victor J (1978) The effect of contrast on the transfer properties of cat retinal ganglion cells. J Physiol (Lond) 285:275–298.
Somers D, Nelson S, Sur M (1995) An emergent model of orientation selectivity in cat visual cortical simple cells. J Neurosci 15:5448–5465.
Stratford K, Tarczy-Hornoch K, Martin K, Bannister N, Jack J (1996) Excitatory synaptic inputs to spiny stellate cells in cat visual cortex. Nature 382:258–261.
Suarez H, Koch C, Douglas R (1995) Modeling direction selectivity of simple cells in striate visual cortex using the canonical microcircuit. J Neurosci 15:6700–6719.
Thomson AM, Deuchars J (1994) Temporal and spatial properties of local circuits in neocortex. Trends Neurosci 17:119–126.
VanEssen D, Anderson C, Fellerman D (1992) Distribution hierarchical processing in the primate cerebral cortex. Science 255:419–423.
Vidyasagar T (1990) Pattern adaptation in cat visual cortex is a cooperative phenomenon. Neuroscience 36:175–179.
Vidyasagar T, Pei X, Volgushev M (1996) Multiple mechanisms underlying the orientation selectivity of visual cortical neurones. Trends Neurosci 19:272–2777.
Zeki S, Shipp S (1988) The functional logic of cortical connections. Nature 335:311–317.